Formation and Decay of Charge Carriers in Bulk Heterojunctions of MDMO-PPV or P3HT with New n-Type Conjugated Polymers

ARTICLE *in* THE JOURNAL OF PHYSICAL CHEMISTRY C · FEBRUARY 2007

Impact Factor: 4.77 · DOI: 10.1021/jp0676540

5 AUTHORS, INCLUDING:

J. Sweelssen
TNO
32 PUBLICATIONS **1,444** CITATIONS
SEE PROFILE

Marc M. Koetse
Solliance/TNO
41 PUBLICATIONS **1,444** CITATIONS
SEE PROFILE

Tom J. Savenije
Delft University of Technology
124 PUBLICATIONS **3,036** CITATIONS
SEE PROFILE

Laurens D A Siebbeles
Delft University of Technology
249 PUBLICATIONS **7,269** CITATIONS
SEE PROFILE

Formation and Decay of Charge Carriers in Bulk Heterojunctions of MDMO-PPV or P3HT with New n-Type Conjugated Polymers

Pieter A. C. Quist,[†] Jörgen Sweelssen,[‡] Marc M. Koetse,[§] Tom J. Savenije,*[,†] and Laurens D. A. Siebbeles[†]

Opto-Electronic Materials Section, DelftChemTech, Faculty of Applied Sciences, Delft University of Technology, Julianalaan 136, NL-2628 BL Delft, The Netherlands, TNO Science and Industry, P.O. Box 6235, 5600 HE Eindhoven, The Netherlands, and Holst Centre/TNO, High Tech Campus 48, 5656 AE Eindhoven, The Netherlands

Received: November 17, 2006; In Final Form: January 10, 2007

The formation and decay of charge carriers in blends of poly(2-methoxy-5-(3′,7′-dimethyloctyloxy)-1,4-phenylene-vinylene) (MDMO-PPV) or poly(3-hexylthiophene) (P3HT) as electron donor with novel n-type electron accepting conjugated polymers, that is, poly(fluorene-bis(1-cyanovinylenethienylene)phenylene) (PF1CVTP) or poly(fluorene-bis(2-cyanovinylenethienylene)phenylene) (PF2CVTP), were studied. Charge carriers were produced by nanosecond pulsed laser excitation, and their decay was monitored by time-resolved microwave conductance measurements. For the blends containing MDMO-PPV, fluorescence spectra and photoconductance data show that excitons decay by efficient electron transfer, possibly preceded by an energy transfer to the component with the lowest band gap. At low laser intensity, the photoconductance per absorbed photon for a blend of MDMO-PPV with PF1CVTP as electron acceptor is approximately four times higher than that for a blend with PF2CVTP as an acceptor, which is probably related to a difference in the morphology of the blend films. At higher intensities, second-order exciton annihilation or charge carrier recombination occurs mainly in short time periods, while in longer time periods, from tens of nanoseconds to milliseconds, charges decay according to first-order kinetics. For blends with P3HT, a lower photoconductance was found than for blends with MDMO-PPV, which is probably due to a lower quantum yield for charge separation.

Introduction

During the past decade, great efforts have been devoted to the development of alternatives for crystalline silicon as a photoactive material in solar cells.[1] A promising approach is the use of organic materials because of their mechanical and chromatic flexibility and their easy and cheap processing. In organic solar cells, photoinduced charge separation is achieved by combining electron donating and accepting materials. Upon absorption of a photon, an exciton is formed, which can dissociate at the interface between the two materials. To be able to contribute to charge carrier formation, excitons must be produced within a distance from the interface that can be overcome by diffusion within their lifetime. To achieve this, bulk heterojunctions (BHJs) are used in which the two components are blended to form a quasi-three-dimensional network.[2,3] A drawback of a BHJ is the enhanced recombination of opposite charges, which occurs in competition with charge diffusion from the blend layer to the electrodes. The nanomorphology of a blend must be realized in such a way that the balance between maximum exciton dissociation and complete charge collection is optimum for solar cell performance.

Several types of BHJs have been investigated for photovoltaic applications. Until now, blends of the conjugated polymer poly(3-hexylthiophene) (P3HT) as electron donor and 1-(3-methoxycarbonyl)-propyl-1-phenyl-(6,6)-C61 (PCBM) as electron acceptor have yielded solar cells with the highest efficiency. Values of 3.5% and even 4.4% under Air Mass (AM) 1.5 have been reported,[4−6] and values up to 5% under AM 1.5 were claimed.[7] Wide band gap metaloxides, such as TiO_2 or ZnO, are also used as electron acceptor. The highest solar cell efficiency reported for this class of materials has been obtained for a BHJ with ZnO and amounts to 1.6%.[8] An important disadvantage of the use of PCBM or metal oxides is the poor absorption in the visible or the near-infrared (NIR) part of the electromagnetic spectrum.

Electron accepting conjugated polymers, which absorb in the visible region, are promising alternatives to PCBM and metal oxides. However, until now only a few electron accepting polymers with potential application in photovoltaic devices have been synthesized.[9−15] One example is a cyano-substituted derivative of poly(2-methoxy-5-(3′,7′-dimethyloctyloxy)-phenylene-vinylene) containing oxygen atoms in the backbone, which exhibited substantial absorption in the visible region.[12] Solar cells based on blends of this material as electron acceptor and poly(2-methoxy-5-(3′,7′-dimethyloctyloxy)-1,4-phenylene-vinylene) (MDMO-PPV) as electron donor showed a clear photovoltaic effect. However, the power conversion efficiency of an optimized device remained limited to 0.75%,[12] probably because of the low electron mobility in the acceptor material. Recently, two new n-type polymers were synthesized, poly(fluorene-bis(1-cyanovinylenethienylene)phenylene) (PF1CVTP) and poly(fluorene-bis(2-cyanovinylenethienylene)phenylene) (PF2CVTP), which differ only by the position where the cyano group is attached (see Figure 1). Their processability is excellent,

* Corresponding author. E-mail: t.j.savenije@tudelft.nl. Tel.: +31 (0)-15 2786537. Fax: +31 (0)15 2787421.
[†] Delft University of Technology.
[‡] TNO Science and Industry.
[§] Holst Centre/TNO.

10.1021/jp0676540 CCC: $37.00
Published on Web 02/28/2007

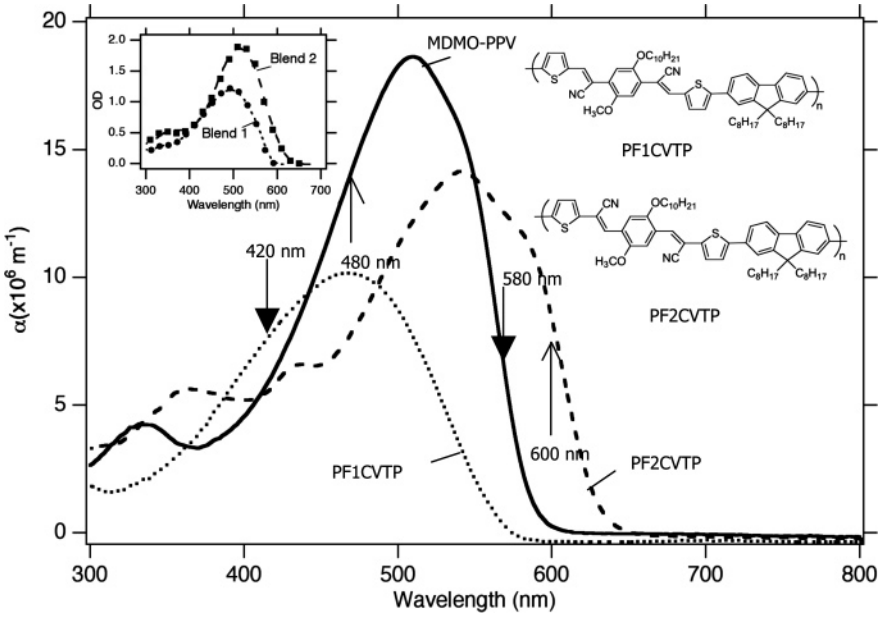

Figure 1. Exponential absorption coefficient as a function of wavelength for MDMO-PPV (solid line), PF1CVTP (dotted), and PF2CVTP (dashed). The arrows indicate the wavelengths used to preferentially excite one of the components of the blend films (closed arrows for blend 1, open arrows for blend 2). The inset shows the optical density spectra for blend 1 (dotted) and blend 2 (dashed). The markers (circles and squares) show the results of fitting a linear combination of the spectra of the individual compounds to that of the blends. The chemical structures of PF1CVTP and PF2CVTP are also shown.

in spite of the absence of ether links in the polymer.[16] By using a BHJ containing MDMO-PPV as electron donor and PF1CVTP as electron acceptor, photovoltaic cells were produced with a power conversion efficiency of 1.5% under AM 1.5 conditions.[16] Although PF2CVTP has a better spectral overlap with the solar spectrum, photovoltaic devices based on blends of this polymer with MDMO-PPV showed significantly lower performances (<1%).[17] Until now, the origin of the different performances of these two electron accepting materials has not been clarified.

The present work aims to provide insight into the processes that determine the photogeneration and decay of charge carriers in blends of MDMO-PPV or P3HT as electron donor and PF1CVTP or PF2CVTP as electron acceptor. Samples were characterized by optical absorption spectroscopy and fluorescence measurements, and the magnitude and decay of the photoconductance were studied by means of time-resolved microwave conductance (TRMC) measurements. The advantage of the TRMC method is that the conductance can be measured without the necessity to apply electrodes to the samples.

Experimental Section

Sample Preparation. MDMO-PPV, synthesized via the sulfinyl route,[18] was used as received. Regioregular P3HT, obtained from Rieke, was purified by reduction with hydrazine, precipitation in methanol, and subsequent Soxhlet extraction in dichloromethane (CH_2Cl_2) and chloroform ($CHCl_3$), yielding a polymer with $M_W = 170.000$ g mol^{-1}. PF1CVTP and PF2CVTP were synthesized according to Cho et al.[19] Details on the polymer properties of MDMO-PPV, PF1CVTP, and PF2CVTP can be found in ref 25.

MDMO-PPV:PF1CVTP, MDMO-PPV:PF2CVTP, P3HT:PF1CVTP, and P3HT:PF2CVTP blend solutions with a total polymer concentration of 11 mg/mL were prepared by dissolving the polymers into chlorobenzene in a 1:1 weight ratio and by stirring for at least 24 h. Blend films were spin-coated onto 1 mm thick, 12 × 25 mm^2 quartz substrates (ESCO products) using a spin speed of 500 rpm for 60 s at room temperature. For optical characterization, films of pure MDMO-PPV, PF1CVTP, and PF2CVTP were spin-coated using the same spin-coating conditions. Samples were prepared under N_2 atmosphere in a glovebox with oxygen concentration < 10 ppm and humidity < 1 ppm. After preparation, all films were annealed for approximately 1 h at $T \approx 135$ °C under N_2 atmosphere to enhance the photoconductance signal. Using a step-profiler with a stylus force of 0.03 mg (Dektak 8, Veeco), we found the thickness of both the MDMO-PPV:PF1CVTP blend film (blend 1) and the MDMO-PPV:PF2CVTP blend film (blend 2) to be 230 nm.

Optical Characterization. A Perkin-Elmer Lambda 900 UV/vis/NIR spectrophotometer equipped with an integrating sphere ("Lab sphere") was used to determine the absorption (OD) and attenuation (F_A) spectra from the fraction of incident light reflected and transmitted by the samples.[20] The exponential absorption coefficient, α, was determined according to $\alpha = \mathrm{OD}\ \ln(10)/L$, where L is the film thickness. A Photon Technology International fluorescence meter was used to obtain the fluorescence spectra of the samples.

Flash-Photolysis Time-Resolved Microwave Conductivity (FP−TRMC). Immediately after preparation, the samples were mounted in an X-band microwave cavity. For photoexcitation, a Nd:YAG laser (Infinity 15-30, Coherent) was used to pump an optical parametric oscillator (OPO), yielding 3 ns full width at half-maximum pulses continuously tunable from 420 to 700 nm. The intensity of the laser beam could be attenuated using a series of metal-coated neutral-density filters (Melles Griot) in tandem, yielding a total number of incident photons per unit area per pulse (I_0) ranging from 10^{11} to 10^{16} photons/cm^2.[20]

Any photoinduced change in the conductance (ΔG) of the sample was monitored as a relative change in the microwave power ($\Delta P/P$) reflected by the cavity using nanosecond time-response microwave circuitry and detection equipment described previously.[20] The results of the TRMC measurements are

expressed in terms of $\Delta G(t)$, which is calculated from $\Delta P/P$ using

$$\Delta G(t) = -\frac{1}{K}\frac{\Delta P(t)}{P} \quad (1)$$

where $K = 1.5 \times 10^4\ \Omega$ is the known sensitivity factor of the cavity containing the sample. The product $\eta\sum_i\mu$, in which $\sum_i\mu$ is the sum of the mobility of a positive and a negative charge carrier and η is the ratio of the number of charge carrier pairs at the maximum of the ΔG transient and the total number of incident photons from the laser pulse, is given by

$$\eta\sum_i\mu = \frac{\Delta G_{max}}{\beta e I_0} \quad (2)$$

where $\beta = 2.1$ corresponds to the ratio of the rectangular dimensions of the waveguide used and e is the elementary charge. The value of $\eta\sum_i\mu$ is divided by the fraction of absorbed photons, F_A, to compare samples with different optical attenuations. The ratio η/F_A is equal to the number of charge carrier pairs per absorbed photon and can be considered as the equivalent of the internal quantum efficiency.

Results and Discussion

Figure 1 shows the wavelength dependence of the exponential absorption coefficients for MDMO-PPV, PF1CVTP, and PF2CVTP with maximum values of $\alpha = 1.9 \times 10^7\ m^{-1}$ at $\lambda = 510$ nm, $\alpha = 1.0 \times 10^7\ m^{-1}$ at $\lambda = 468$ nm, and $\alpha = 1.4 \times 10^7\ m^{-1}$ at $\lambda = 540$ nm, respectively. The electron accepting polymers strongly absorb visible light in contrast to the commonly used electron acceptors such as PCBM and metal oxides. The inset shows the optical density spectra for 230 nm thick MDMO-PPV:PF1CVTP and MDMO-PPV:PF2CVTP blend films, hereafter denoted as blend 1 and blend 2, respectively. Fits of a linear combination of the wavelength dependent absorption coefficients of the individual components to the spectra of the blends are also shown. Best fits are obtained using ratios of 1:1.3 (MDMO-PPV:PF1CVTP) and 1.5:1 (MDMO-PPV:PF2CVTP). It is clear from Figure 1 that both polymers in the blends have a substantial absorption in the visible light region, so that absorption of visible light leads to the formation of excitons in both polymers. However, for blend 1, preferential excitation of the electron acceptor can be realized at 420 nm, while the electron donor can be preferentially excited at 580 nm. For blend 2, the electron acceptor can be preferentially excited at 600 nm, and the electron donor can be preferentially excited at 480 nm.

Fluorescence spectra obtained upon excitation at 510 nm, corresponding with the absorption maximum of MDMO-PPV, are shown in Figure 2 for blends containing MDMO-PPV as electron donor and for the individual components. The fluorescence is substantially quenched in the blend films, with the effect being largest for blend 2. This provides evidence that by mixing the components of the two blends an additional decay pathway for the excitons is formed, that is, charge transfer. The stronger fluorescence quenching in blend 2 may indicate a morphology with a more intimate mixing of the two components than in blend 1 so that, on average, in blend 2 the excitons are formed closer to the donor/acceptor interface. In blends with P3HT as electron donor (data not shown), the fluorescence is quenched to a much lesser extent.

The fluorescence spectra of blend 1 in the inset of Figure 2A were obtained on the preferential excitation of MDMO-PPV (in this case at 510 nm, because at 580 nm the absorption is too poor) or PF1CVTP (at 420 nm). The spectra resemble each other and are similar to that for a layer of MDMO-PPV alone. This indicates that for blend 1 the remaining fluorescence is due to the decay of excitons in MDMO-PPV. The fluorescence spectra of blend 2 in the inset of Figure 2B, obtained on the preferential excitation of MDMO-PPV (480 nm) or PF2CVTP (600 nm), are almost identical and have a shape similar to that for PF2CVTP. It is inferred from this that the fluorescence for blend 2 stems from PF2CVTP for both excitation wavelengths. The fluorescence data suggest that efficient exciton transfer occurs to the material with the lowest band gap (see Figure 1), that is, from PF1CVTP to MDMO-PPV in blend 1 and from MDMO-PPV to PF2CVTP in blend 2. Note that the maximum in the fluorescence spectrum of blend 2 is red-shifted from $\lambda \approx 650$ nm for PF2CVTP to $\lambda \approx 700$ nm for the blend. This shift could be due to the fact that interchain interactions and polymer chain conformations of PF2CVTP in the blend differ from those in the pure material.

Figure 3 shows the microwave conductance transients for blend 1 and blend 2 and for films of the individual components on photoexcitation near their absorption maxima. Clearly, a much larger and longer-lived signal is observed for the blend layers than for films of the individual components, indicating that charge generation is much more efficient in blend films. The initial rise time of the photoconductance largely exceeds the laser pulse duration of 3 ns, which is due to the 18 ns time response of the microwave cavity cell used. After reaching a maximum at approximately 20−30 ns after the laser pulse, the microwave conductance decays as a result of trapping or recombination of charge carriers, or both. For blend 1, the decay of the photoconductance is somewhat faster than for blend 2. Note that the origin of the decay of the microwave conductance differs from the cause of the current decay in, for example, time-of-flight (TOF) measurements, which is due to the collection of charges by the electrodes.

Figure 4A shows the photoconductance transients on preferential excitation of the donor in blend 1 at 580 nm for various laser intensities. Similar results were found for the preferential excitation of the acceptor at 420 nm and for excitation at 510 nm. On times exceeding the cavity response time, the decay does not depend much on the laser intensity. Hence, photoinduced charge carriers decay mainly via first-order processes rather than by second-order recombination. In addition, the decay of the photoconductance of blend 2 for excitation at 480, 510, or 600 nm was also found to be almost independent of the laser intensity (data not shown). The photoconductance decays according to a power law, $\Delta G \propto t^{-\gamma}$, with $\gamma = 0.35$ for blend 1 and with $\gamma = 0.29$ for blend 2. These values for γ are very close to the value found earlier for the relaxation of holes on MDMO-PPV.[21] This also suggests, in this work, that the largest contribution to the photoconductance is formed by the holes. Decay according to a power law is typical for relaxation of charge carriers in a disordered energy landscape with an exponential distribution of the energy of the localization sites.[22] Formation of triplets (eventually via excimers) can also form a decay pathway for the charge carriers.[23−25]

Figure 4B shows the values of $\eta\sum_i\mu/F_A$, defined in eq 2, as obtained from the maxima in the $\Delta G(t)$ transients for the blend films upon photoexcitation at 510 nm, that is, at the absorption maximum of the electron donor MDMO-PPV. For low laser intensities, the magnitude of the photoconductance is proportional to I_0, and the quantity $\eta\sum_i\mu/F_A$, as shown in Figure 4B, is independent of the intensity.

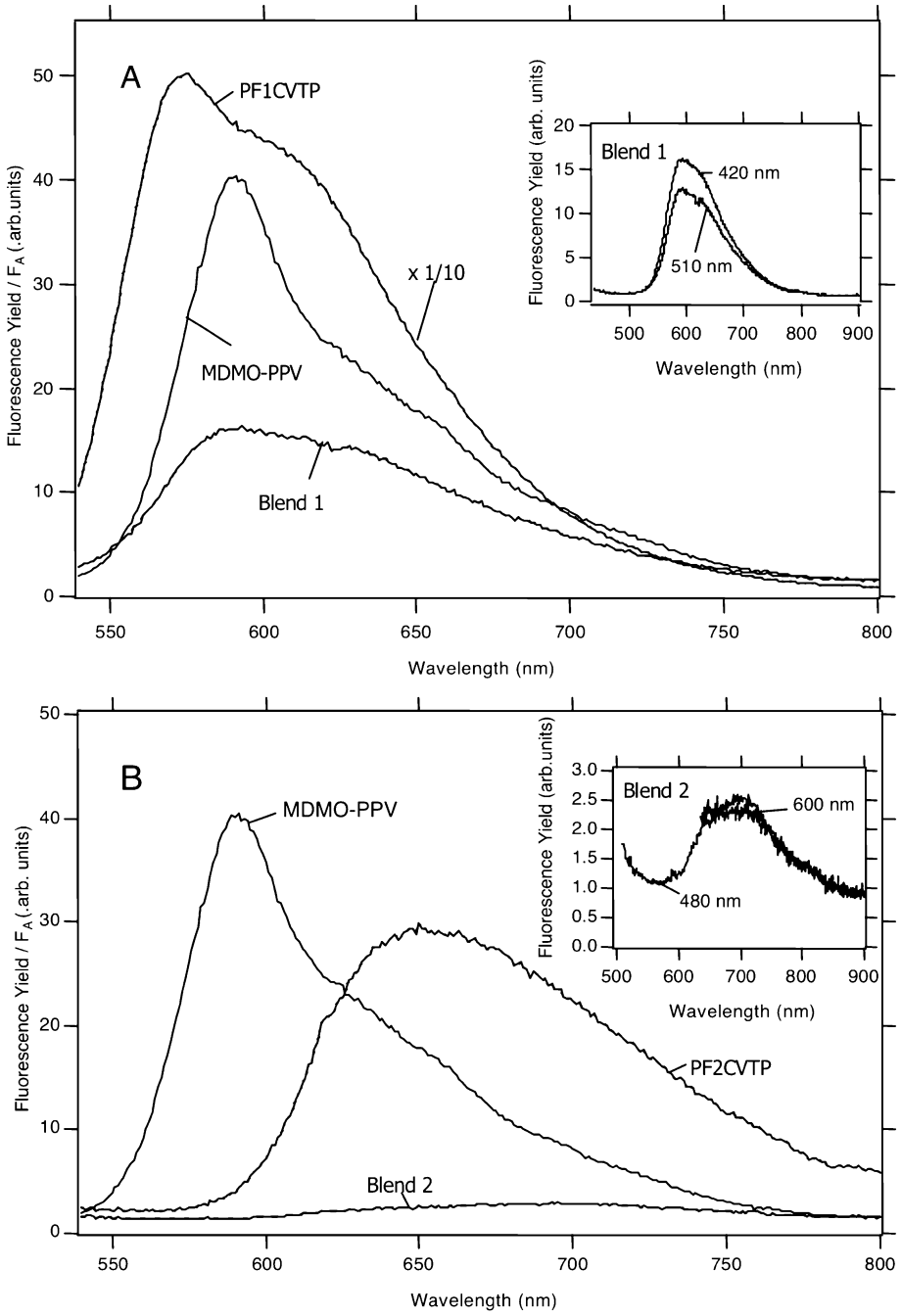

Figure 2. Fluorescence spectra for blend films and films of the individual compounds. (A) MDMO-PPV, PF1CVTP, and blend 1. (B) MDMO-PPV, PF2CVTP, and blend 2. The insets show the fluorescence spectra for blend 1 (A) and blend 2 (B) on excitation at different wavelengths: (A) 420 nm and 510 nm and (B) 480 nm and 600 nm.

At higher laser intensities the observed photoconductance is proportional to the incident laser power raised to a power δ, that is, $\Delta G \propto I_0^{\delta}$ with $\delta = 0.4$ and $\delta = 0.5$ for blend 1 and blend 2, respectively. This sub-linear behavior is due to second-order processes like exciton−exciton annihilation, bimolecular charge recombination, or both. Because of the limited time resolution of our setup, we cannot quantify to what extent these two processes contribute to the gradual lowering of $\eta\sum\mu/F_A$ for higher laser intensities. However, on time scales below 40 ns, the dependence of the decay kinetics of the photoconductance on the laser intensity demonstrates that at least a part of the charge carriers recombine by a second-order process.

The maximum $\eta\sum\mu/F_A$ value of 0.02 $cm^2/(V\ s)$ found for blend 1 is very similar to the value reported earlier for a blend of MDMO-PPV with a different n-type polymer.[21] In that work, it was concluded that the photoconductance was predominantly due to mobile holes. The similarity between the observed $\eta\sum\mu/F_A$ values indicates again that in blend 1 the photoconductance is dominated by holes in MDMO-PPV.

The data in Figure 4B show that at low intensities, where second-order recombination processes do not play a significant role, $\eta\sum\mu/F_A$ is about a factor of 4 higher for blend 1 than for blend 2. Interestingly, this observation corresponds with the finding that solar cells based on blend 1 perform better than those based on blend 2, despite the fact that the absorption spectrum of blend 2 has a better overlap with the solar emission spectrum. The difference in $\eta\sum\mu/F_A$ must be due to different charge carrier mobilities, $\sum\mu$, a different yield of free charges per absorbed photon for the two blends, η/F_A, or both. The mobility of charge carriers is determined by the confirmation

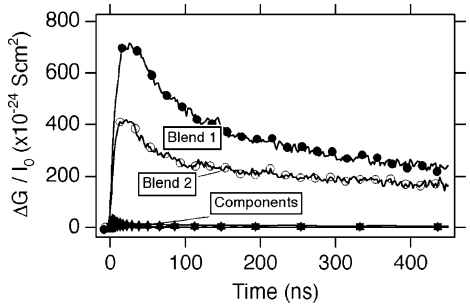

Figure 3. Microwave conductance transients normalized to the incident laser intensity for films of the individual compounds and for the blends: MDMO-PPV (triangles), PF1CVTP (inverted triangles), PF2CVTP (diamonds), blend 1 (closed circles), and blend 2 (open circles). The films were excited near their absorption maxima: $\lambda =$ 500 nm (MDMO-PPV), $\lambda = 450$ nm (PF1CVTP), and $\lambda = 530$ nm (PF2CVTP). The blend films were excited at $\lambda = 510$ nm.

of the polymer chains, which depends on the film morphology. The yield of free charges is determined by both the yield of exciton dissociation and the yield of escape of charges from geminate recombination. A morphology with a more intimate mixture of the components may enhance the extent of exciton dissociation, since a larger fraction of the excitons will reach the polymer/polymer interface within their lifetime. On the basis of the fluorescence measurements discussed above, it was inferred that blend 1 exhibits a less intimate mixing, which is expected to lead to a lower exciton dissociation yield. The observation, nevertheless, that the photoconductivity is higher for blend 1 can be due to a higher yield of escape of charges from geminate recombination. For blend 1, the more phase separated morphology with larger domains of the donor and the acceptor can facilitate the escape of the charges from geminate recombination, as was found earlier for a blend of MDMO-PPV with a different n-type polymer.[21] Morphology studies such as electron energy loss spectroscopy (EELS) in combination with energy-filtering transmission electron microscopy (EFTEM)[26] and terahertz conductivity experiments that allow monitoring of the photoconductance in the picosecond time domain may clarify this issue.

The action spectrum for blend 1 is shown in Figure 4C, together with the optical attenuation spectrum. The action spectrum is expressed in $\eta\sum\mu$ instead of $\eta\sum\mu/F_A$ to facilitate comparison of the spectra. The similar shape of the action and attenuation spectra indicates that the efficiency of charge carrier generation is independent of excitation wavelength. The latter was also found for blend 2 (data not shown). Hence, excitation of the donor or the acceptor is equally efficient for charge carrier generation. This can be interpreted in two ways: (I) Electron transfer following excitation of the donor occurs with an efficiency equal to hole transfer upon excitation of the acceptor. (II) Prior to exciton dissociation in free charge carriers, energy transfer occurs to the polymer with the lowest band gap, followed by transfer of an electron (blend 1) or hole (blend 2). These two different routes are depicted in Figure 5. The fluorescence spectrum of blend 2 (see Figure 2) resembles that of PF2CVTP and is independent of the excitation wavelength (see inset Figure 2B). On the basis of these observations, route II is considered most likely for blend 2.

For blend films with P3HT as electron donor and PF1CVTP or PF2CVTP as acceptor, the values found for $\eta\sum\mu/F_A$ were lower than those found with MDMO-PPV as donor. This finding agrees with the lower performance of solar cells with P3HT as electron donor, as compared with the solor cells containing MDMO-PPV as donor.[27] In addition, the $\eta\sum\mu/F_A$ values were

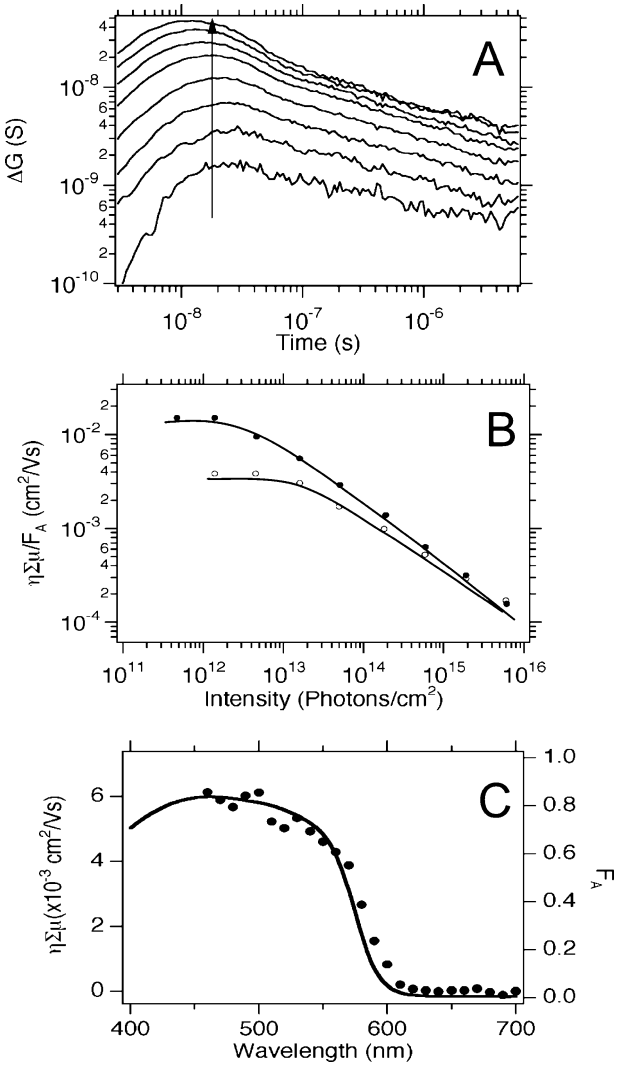

Figure 4. (A) Photoconductance transients on excitation of blend 1 at $\lambda = 580$ nm with different laser pulse intensities, increasing in the direction of the arrow. The intensity values are 2.4×10^{12}, 7.7×10^{12}, 1.9×10^{13}, 6.3×10^{13}, 2.0×10^{14}, 6.5×10^{14}, 2.1×10^{15}, and 6.9×10^{15} photons/cm^2 per pulse. (B) $\eta\sum\mu/F_A$ as a function of the intensity of photoexcitation at $\lambda = 510$ nm of blend 1 (closed circles) and blend 2 (open circles). The lines are guides for the eye. Note that $\eta\sum\mu/F_A$ is constant at lower intensity. (C) Action spectrum (circles) and attenuation spectrum (line) of blend 1. The laser pulse intensity was ca. 10^{13} photons/cm^2 per pulse.

found to decrease over the entire range of laser intensities used, and the corresponding sub-linear increase of the photoconductance is characterized by $\Delta G \propto I_0^{\delta}$ with $\delta = 0.5$. For even lower intensities, the signal-to-noise ratio became too low. The lower $\eta\sum\mu/F_A$ values for the blends with P3HT as electron donor can be explained, in principle, by a lower charge carrier mobility, by a lower yield of charge carriers, or by both. It has been reported in the literature that the mobility of holes in blends of P3HT with PCBM[28] is much higher than that in blends of MDMO-PPV with PCBM.[29] If, for the present blends, the mobility of holes is also higher for P3HT than for MDMO-PPV, then the lower photoconductivity for blends with P3HT must be due to a lower charge carrier yield. Our observation that the fluorescence in blends with P3HT as electron donor is quenched to a lesser extent than in those with MDMO-PPV as donor corroborates the latter. Possibly, the smaller extent of quenching results from a relatively small exciton diffusion length

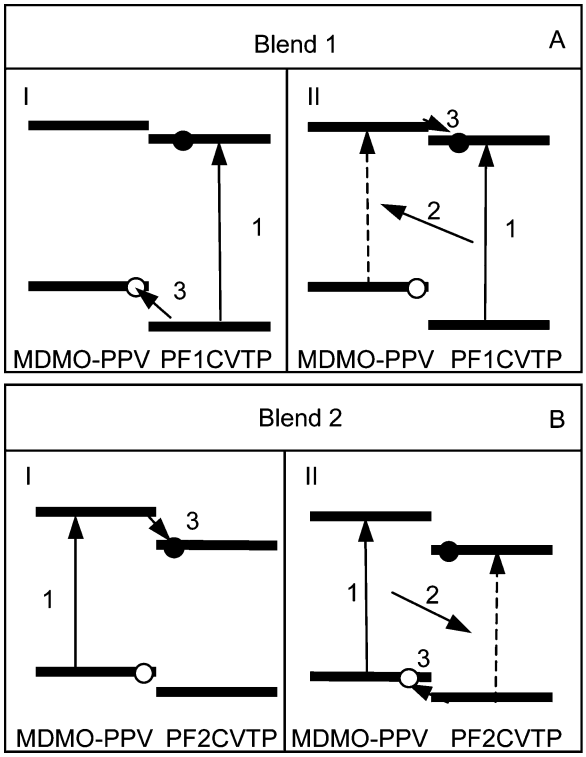

Figure 5. Schematic representation of possible photophysical processes (routes I and II). Panel A is for blend 1, and panel B is for blend 2. The left panels (route I) represent excitation of donor or acceptor (1) followed by charge transfer (3). The right panels (route II) represent excitation of the component with the largest band gap (1) followed by energy transfer (2) and consecutive charge transfer (3).

in P3HT,[20] in combination with a less intimate mixture of P3HT with the electron accepting polymers.

Conclusions

Charge carrier dynamics in blends with MDMO-PPV as electron donor and PF1CVTP or PF2CVTP as electron acceptor has been studied. Fluorescence quenching in the blends is attributed to the dissociation of excitons into free charge carriers. By combining the results from optical absorption, fluorescence, and action spectra, it was inferred that exciton transfer to the polymer with the lowest band gap occurs prior to exciton dissociation.

At a low laser pulse intensity, the product of the charge generation efficiency per absorbed photon and the sum of the charge carrier mobilities ($\eta\sum\mu/F_A$) were determined to be 0.02 $cm^2/(V\ s)$ for blend 1 and 0.005 $cm^2/(V\ s)$ for blend 2. The higher value for blend 1 agrees with the finding that solar cells based on this blend perform better than those based on blend 2 and is probably related to a more favorable morphology of the former blend film. At higher intensities, the photoconductance of the blend films increases sub-linearly with the laser pulse intensity, which is characteristic for second-order processes. On longer time scales, charges decay according to a first-order process.

The photoconductance for blends with P3HT as donor was found to be lower than that for blend films with MDMO-PPV as donor. This is in accordance with the poor cell performance of solar cells based on P3HT:PF1CVTP and P3HT:PF2CVTP blend films and the smaller amount of fluorescence quenching in these blend films as compared with those with MDMO-PPV as donor. These observations indicate a low quantum yield for charge carrier generation, possibly caused by a poor mixing of donor and acceptor polymers.

Acknowledgment. This work is part of the program Polymer Photovoltaics (DPI 323 and 325) of the Dutch Polymer Institute (DPI). The work of P.A.C.Q., J.S., and M.M.K. forms part of the research program of the Dutch Polymer Institute.

References and Notes

(1) Brabec, C.; Dyakonov, V.; Parisi, J.; Sariciftci, N. S. *Organic Photovoltaics Concepts and Realization;* Springer: Heidelberg, Germany, 2003.
(2) Sariciftci, N. S.; Smilowitz, L.; Heeger, A. J.; Wudl, F. *Science* **1992**, *258*, 1474.
(3) Yu, G.; Gao, J.; Hummelen, J. C.; Wudl, F.; Heeger, A. J. *Science* **1995**, *270*, 1789.
(4) Padinger, F.; Rittberger, R. S.; Sariciftci, N. S. *Adv. Funct. Mater.* **2003**, *13*, 85.
(5) Li, G.; Shrotriya, V.; Huang, J. S.; Yao, Y.; Moriarty, T.; Emery, K.; Yang, Y. *Nat. Mater.* **2005**, *4*, 864.
(6) Kim, Y.; Cook, S.; Tuladhar, S. M.; Choulis, S. A.; Nelson, J.; Durrant, J. R.; Bradley, D. D. C.; Giles, M.; McCulloch, I.; Ha, C. S.; Ree, M. *Nat. Mater.* **2006**, *5*, 197.
(7) Brabec, C. J. *Sol. Energy Mater. Sol. Cells* **2004**, *83*, 273.
(8) Beek, W. J. E.; Wienk, M. M.; Kemerink, M.; Yang, X.; Janssen, R. A. J. *J. Phys. Chem. B* **2005**, *109*, 9505.
(9) Egbe, D. A. M.; Kietzke, T.; Carbonnier, B.; Muhlbacher, D.; Horhold, H. H.; Neher, D.; Pakula, T. *Macromolecules* **2004**, *37*, 8863.
(10) Manoj, A. G.; Alagiriswamy, A. A.; Narayan, K. S. *J. Appl. Phys.* **2003**, *94*, 4088.
(11) Takahashi, K.; Seto, K.; Yamaguchi, T.; Nakamura, J.; Yokoe, C.; Murata, K. *Chem. Lett.* **2004**, *33*, 1042.
(12) Veenstra, S. C.; Verhees, W. J. H.; Kroon, J. M.; Koetse, M. M.; Sweelssen, J.; Bastiaansen, J.; Schoo, H. F. M.; Yang, X.; Alexeev, A.; Loos, J.; Schubert, U. S.; Wienk, M. M. *Chem. Mater.* **2004**, *16*, 2503.
(13) Yu, G.; Heeger, A. J. *J. Appl. Phys.* **1995**, *78*, 4510.
(14) Zhang, F. L.; Jonforsen, M.; Johansson, D. M.; Andersson, M. R.; Inganas, O. *Synth. Met.* **2003**, *138*, 555.
(15) Halls, J. J. M.; Walsh, C. A.; Greenham, N. C.; Marseglia, E. A.; Friend, R. H.; Moratti, S. C.; Holmes, A. B. *Nature* **1995**, *376*, 498.
(16) Koetse, M. M.; Sweelssen, J.; Hoekerd, K. T.; Schoo, H. F. M.; Veenstra, S. C.; Kroon, J. M.; Yang, X. N.; Loos, J. *Appl. Phys. Lett.* **2006**, *88*.
(17) Koetse, M. M.; Veenstra, S. C. Unpublished results, 2005.
(18) Lutsen, L.; Adriaensens, P.; Becker, H.; Van Breemen, A. J.; Vanderzande, D.; Gelan, J. *Macromolecules* **1999**, *32*, 6517.
(19) Cho, N. S.; Hwang, D. H.; Jung, B. J.; Lim, E.; Lee, J.; Shim, H. K. *Macromolecules* **2004**, *37*, 5265.
(20) Kroeze, J. E.; Savenije, T. J.; Vermeulen, M. J. W.; Warman, J. M. *J. Phys. Chem. B* **2003**, *107*, 7696.
(21) Quist, P. A. C.; Savenije, T. J.; Koetse, M. M.; Veenstra, S. C.; Kroon, J. M.; Siebbeles, L. D. A. *Adv. Funct. Mater.* **2005**, *15*, 469.
(22) Siebbeles, L. D. A. *Chem. Phys. Lett.* **1997**, *265*, 460.
(23) Morteani, A. C.; Sreearunothai, P.; Herz, L. M.; Friend, R. H.; Silva, C. *Phys. Rev. Lett.* **2004**, *92*.
(24) Offermans, T.; van Hal, P. A.; Meskers, S. C. J.; Koetse, M. M.; Janssen, R. A. J. *Phys. Rev. B: Condens. Matter Mater. Phys.* **2005**, *72*.
(25) Veldman, D.; Offermans, T.; Sweelssen, J.; Koetse, M. M.; Meskers, S. C. J.; Janssen, R. A. J. *Thin Solid Films* **2006**, *511*, 333.
(26) Loos, J.; Yang, X. N.; Koetse, M. M.; Sweelssen, J.; Schoo, H. F. M.; Veenstra, S. C.; Grogger, W.; Kothleitner, G.; Hofer, F. *J. Appl. Polym. Sci.* **2005**, *97*, 1001.
(27) Koetse, M. M. Unpublished results, 2005.
(28) Savenije, T. J.; Kroeze, J. E.; Yang, X. N.; Loos, J. *Adv. Funct. Mater.* **2005**, *15*, 1260.
(29) Melzer, C.; Koop, E. J.; Mihailetchi, V. D.; Blom, P. W. M. *Adv. Funct. Mater.* **2004**, *14*, 865.